of position (9,1) when the large probe is used. Hence, the boundary layer should be laminar, and measurements taken with a flattened hypodermic impact probe verified that the boundary-layer width was that expected for a laminar layer. The largest wall interference to be expected is that at station (9,1) with the lowest value of Reynolds number, (8×10^4), which corresponds to a displacement thickness-to-probe-diameter ratio of 0.05, and corresponding flow angularity at the boundary-layer edge of 0.2 deg. These values were taken to be inconsequential in their effect upon the probe readings. The boundary-layer-edge flow angularity at position (1,1) was calculated as 0.5 deg, which could have a measurable but not dominant effect at the probe location. The experimental apparatus used in this part of the experiment was exactly the same as used during the calibration procedure with the addition of the flat plate and its fixture. Once again the true angles were compared to the computed angles.

The sideslip angle behavior was quite similar to that obtained for the case with no sidewall present, with no persistent wall influence becoming evident. In the case of the angle-of-attack behavior, however, although the data scatter was similar to that previously obtained, a substantial and persistent shift in mean angle of attack was found (Fig. 2).

The shift in the mean is termed herein the estimated increment, and denoted by the symbol Δ_β. The least-squares-averaged results for the four probe positions and three probe configurations, as well as the related estimated increments, are shown in Table 1. As is to be expected, the estimated increment in angle of attack decreased with increasing distance from the solid surface. The data reveal that the estimated increment in angle of attack reduces with increased rearward positioning of the probe [compare probes (1,1) and (9,1)]. It appears that this discrepancy is identified with a slight lifting interference caused by the wind tunnel walls above the flat plate introducing slight flow diffusion.

Summary and Conclusions

A calibration method to determine the sideslip angle and angle of attack with five-hole probes was developed and applied to a series of test cases.

The probe behavior was then studied in several positions relative to a flat plate. As expected, the probe overreading of angle of attack increased with increased approach to the wall. The wall interference causes an increased pressure at port 2, which in turn leads to an increase in estimated angle of attack. The estimated increment in angle of attack found in close proximity of the wall substantially exceeded the standard deviation of errors identified with the calibration procedure. From this it is concluded that the validity of probe readings can be extended to within wall influence regimes by including the effect of wall interaction in the calibration procedures. As a rough approximation, the estimated increments obtained in this investigation could be utilized directly in other studies, provided geometric similarity between probes is preserved. It must be noted, however, that this investigation was deliberately conducted to investigate wall influence without the presence of substantial shears. The issue of the effects of boundary layers or separated regions is not addressed.

Acknowledgments

This work was supported by Grant AFOSR-80-0186G from the U.S. Air Force Office of Scientific Research.

References

[1]Barker, K.W., Gallington, R.W., and Minster, S.N., "Calibration of Five-Hole Probe for On-Line Data Reduction," USAFA-TR-79-7.

[2]Gerner, A.A. and Maurer, C.L., "Calibration of Seven-Hole Probes Suitable for High Angles in Subsonic Compressible Flows," AIAA Paper 82-0410, 1982.

[3]Tamigniaux, T.L.B., "An Experimental Investigation of the Wall-Effect on a Five-Hole Pressure Probe," Master of Engineering Thesis, University of Washington, Seattle, March 1984.

Cavity Flow Control for Supersonic Lasers

Wolfgang O. Schall*
DFVLR Institut für Technische Physik
Stuttgart, Federal Republic of Germany

Introduction

BOUNDARY-layer separation in a flow across a deep cavity such as a resonator opening in a flowing gas laser, can be a source of large density inhomogeneities. Producing laser outputs with high-quality beams requires small phase distortions and hence small density variations, $\Delta\rho/\rho$, of the medium. For certain molecular lasers, $\Delta\rho/\rho$ may not exceed 1%. This corresponds to a pressure variation of $\Delta p/p=\gamma\Delta\rho/\rho$ for weak waves in supersonic flows, where γ is the specific heat ratio. Petty et al.[1] and Shen[2] investigated the flowfield of a supersonic duct flow over several cavity shapes. Shen attempted to eliminate flow separation by contouring the edges of the cavity. The importance of edge contours on the achievable beam power in a supersonic CO laser has been confirmed by Schall,[3] who subsequently studied this phenomenon in more detail on resonator cavities.[4]

If a significant reduction of the waves induced by the boundary layer can be achieved, then other applications of cavities in flowing lasers may be possible. For instance, the heat deposited in the cathode sheath of a supersonic discharge laser creates a thickening of the electrode boundary layer, which in turn causes a compression wave of several percent pressure jump at the electrode leading edge.[5] The retraction of the electrodes from the wall into a cavity, together with a suitable shear layer control, could greatly reduce the strength of such waves.[6] In this Note, the effects of controlled variations in cavity gas temperatures and pressures on well-ordered wave strength in the main flow will be reported.

Experimental Studies and Results

A flow channel with a 14.4×25 mm^2 cross section was used in all of the experiments. See Fig. 1. Two openings in the top and bottom wall allowed for the insertion of different edge configurations and cavity designs. The aperture of the cavity opening was fixed at 25×26 mm^2 and the depth of the cavity was held at 40 mm. The sidewalls of the duct were equipped with windows to allow schlieren photography. Based on an estimated wave thickness (order of 10^{-7} m) and a focal length of 0.5 m, the density resolution of the schlieren system was better than 0.5% ($\delta\rho/\rho$), allowing waves from wall steps of $\sim$0.01 mm to be seen. The static pressure was measured at the top wall 40 mm ahead of the center of the cavity opening p_1 and at the cavity wall p_c. Pressure gradients within the cavity were sufficiently small to allow selection of p_c as the characteristic cavity value. For the measurement of pressure profiles across the flow, one window could be replaced by a plate with pressure taps. The pressure resolution was better than 1 mbar (100 Pa) and pressure values of independent runs could be reproduced to within 2.5 mbar. Nitrogen, at a flow rate of 93.5 g/s, was accelerated to Mach number 3.5 at $p_1=100$ mbar. The flow was turbulent with a Reynolds number of 2.5×10^6 and a boundary-layer thickness of 2.75 mm at the cavity leading edge.

Two designs of the edges of the cavity opening were used in the tests. The first was a standard insert with rectangular

Received July 27, 1984; revision submitted March 20, 1985.

*Research Scientist and Groupleader. Member AIAA.

edges. It produced an overpressure inside the cavity of ~5% compared to the main flow pressure immediately in front of the boundary-layer separation wave. The overpressure was caused by the diversion of a small part of the shear layer into the cavity. Compression waves were created at the separation point and at the downstream edge of the cavity. The shear layer reattached to the downstream wall with a moderate pressure increase of 15% across the cavity opening. A second insert had a rounded shoulder upstream with a 6 mm radius of curvature and a lip downstream with 20 deg ramp angle. This insert produced a drop in p_c by ~5%. However, the ramp caused a strong deflection of the shear layer into the main flow, resulting in a total pressure increase of nearly 100% across the cavity opening.

In a first experiment, thermal energy was deposited inside the cavity by resistively heating a mesh of wound constantan wire. The mesh was placed 16 mm below the channel wall and did not recognizably alter the state of the cavity flow. Figure 2 shows the relative pressure increase in the cavity as a function of the thermal power load. The maximum applied power of 15 W corresponds to a power density of 2.3 W/cm^2 with respect to the cavity opening. The weak pressure increase is linear (except for very small powers) and is not noticeable on the schlieren picture. It corresponds to but a few degrees centigrade temperature rise in the cavity gas. The strong turbulent eddy motion inside the cavity[4] provides a strong heat exchange with the walls. Furthermore, a diversion of mass into the cavity requires a heat and mass exchange across the shear layer, explaining the somewhat lower pressures for the standard cavity configuration. The temperature change in the cavity gas does not appear to be very efficient for influencing the pressure field.

On the other hand, a screen electrode placed in a cavity would also dissipate its excess heat within the cavity. The minor effect upon the shear layer could then be controlled by other means, including cooling of the cavity walls. At equal pressures, a resting or slowly flowing gas can sustain a higher energy loading than a supersonically flowing gas before it breaks down.[7] Hence, arcing problems would not be enhanced because the cavity density is not lower than the density in the heated boundary layer of a channel wall electrode. Not considered in this discussion is the significant density gradient that a discharge transverse to the flow produces in the flow direction, which could considerably alter the flow pattern.

A better method for influencing the pressure inside the cavity is the addition or removal of mass. In resonators a purge gas flow is often used to protect the laser mirrors from contamination or corrosion. Mass addition through the cavity turns out to be very detrimental for the homogeneity of the flow, even at low flow rates. Figure 3 shows the strong rise in the relative cavity pressure with increasing injection rate $\dot{m}_c$.

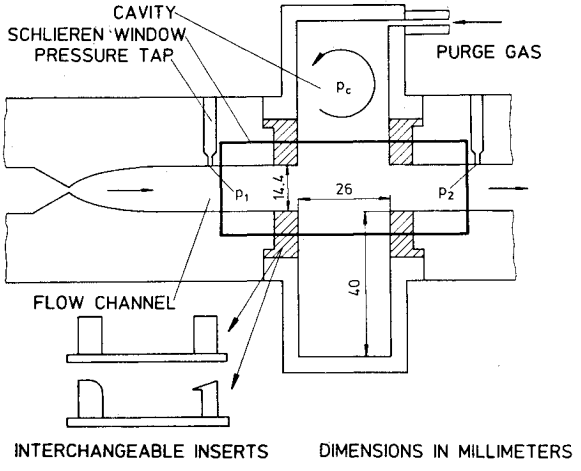

Fig. 1 Schematic diagram of experimental apparatus.

The shear layer bulges into the main flow, resulting in a compression wave at the upstream cavity edge. For 0.5 g/s, the reattachment of the shear layer is shifted beyond the downstream cavity edge. With $\dot{m}_c > 1$ g/s, the separation point starts moving upstream from the cavity leading edge. The shear layer continues to bridge across the cavity, expanding to approximately 3 g/s, but p_c increases by 100%. For even higher $\dot{m}_c$, the shear layer is turned sharply into the core flow where it mixes within a few centimeters. This behavior is fairly independent of the edge design.

The pressure curve can be readily extended to negative mass flows or gas suction. Suction allows p_c to be reduced below the freestream pressure. For these particular experiments, a zero pressure difference with respect to p_1 was found for a suction rate of 0.49 g/s. Pressure matching with a vanishing separation wave should have been obtained for 0.12 g/s suction. However, the leading-edge wave could not be made to disappear on the schlieren picture for either flow rate.

Although mass removal can reduce cavity-induced pressure gradients into the core flow, it increases the generally undesired entrainment of laser gas into the cavity. In situations where cavity purging is indispensable, the excess pressure

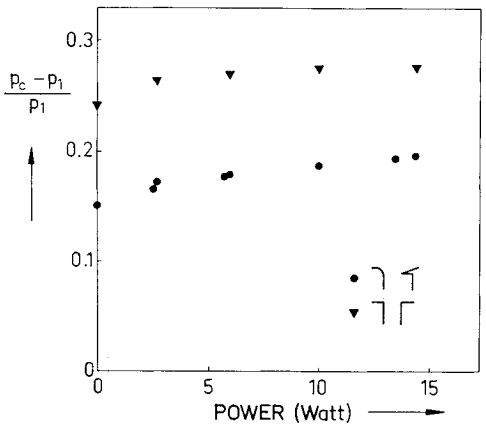

Fig. 2 Relative pressure change with heating rate inside the cavity.

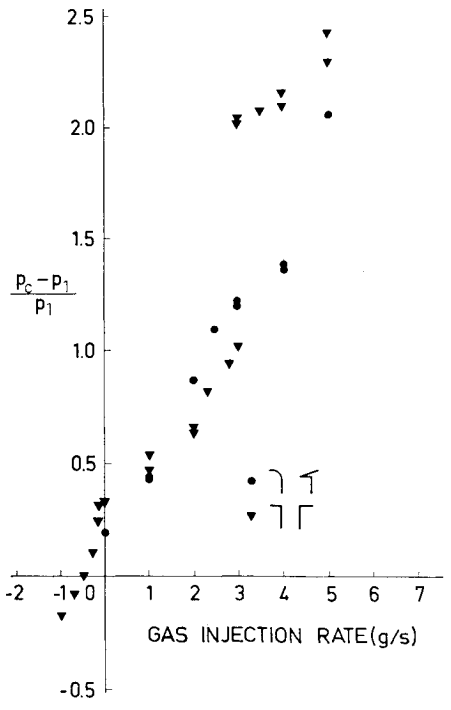

Fig. 3 Relative pressure change with mass addition to the cavity.

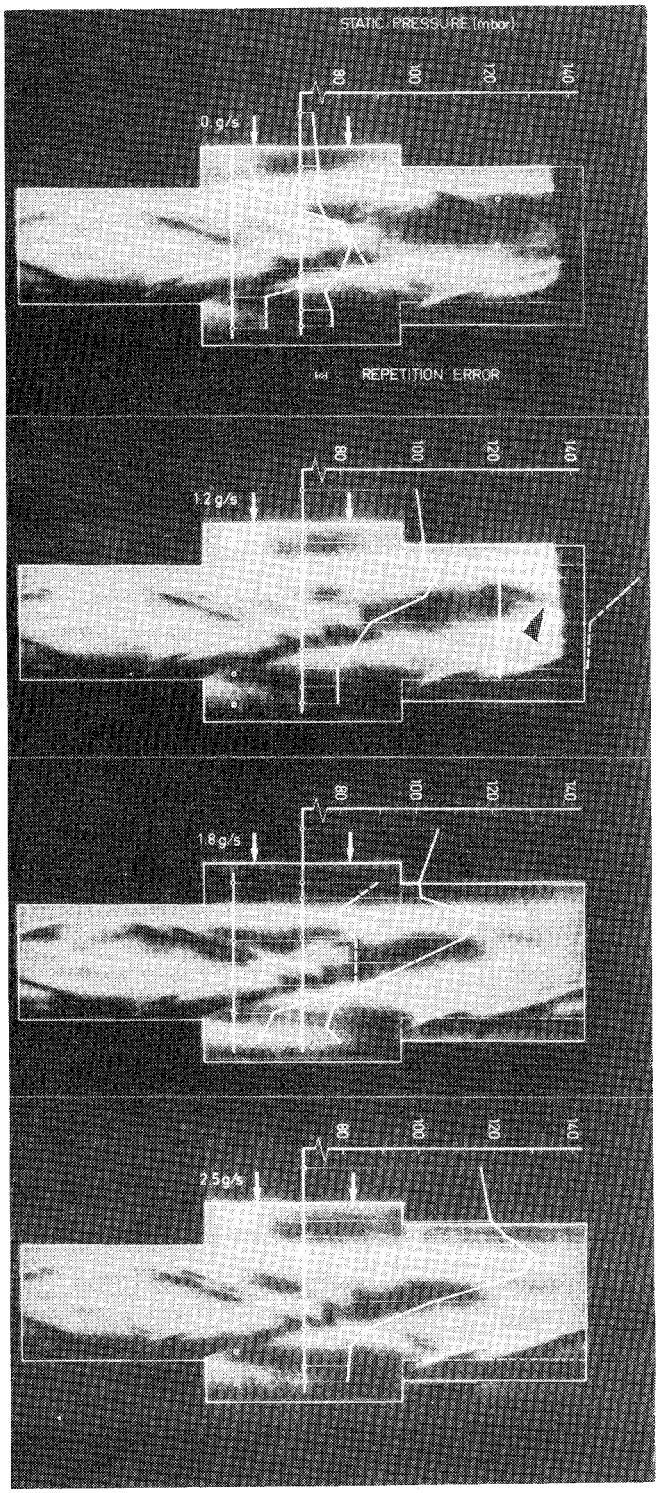

Fig. 4 Schlieren picture and pressure distribution of the supersonic channel flow if gas is injected into the upper cavity at an increasing rate, as indicated by arrow (horizontal knife edge from above).

must be compensated for by other means. This can be achieved by enlarging the channel cross section downstream of the cavity by an appropriate ratio. Slight changes in the flow rate of the purge gas can then be used to fine tune the cavity pressure level to a value where the separation wave is minimized.

In a further set of experiments, the channel height downstream of the cavity opening was enlarged by 6 mm. The purge gas was blown into the cavity parallel to the cavity bottom and in the turning direction of the cavity vortex (Fig. 1). As conjectured, the change of $(p_c - p_1)/p_1$ as a function of $\dot{m}_c$ was nearly independent of the inserts used. A flow rate of 0-2.5 g/s covered a pressure change of $\pm 20\%$. However, only the standard insert produced a shear layer of satisfactory straightness. Here, the schlieren pictures indicate a transition from an expanding to a contracting main flow with an intermediate state where no visible wave emanates from the separation point. Figure 4 shows this in a sequence of schlieren photographs with increasing $\dot{m}_c$. Gas was injected into the upper cavity only. As long as the cavity mass flow injection rate is zero, the shear layer bends toward the cavity opening due to the expanding main flow. A rarefaction fan emanates from the separation edge and a weak compression wave is produced at the reattachment point. For $\dot{m}_c = 1.2$ g/s, where $(p_c - p_1)/p_1 = 0$, the shear layer exhibits a wavy nature and a rarefaction wave is still produced. It disappears entirely at $\dot{m}_c = 1.8$ g/s. The shear layer now remains virtually parallel to the channel wall down to the very end of the window. For even higher flow rates, the shear layer bends toward the channel center and a weak compression wave develops.

Superimposed on the photographs of Fig. 4 are static pressure profiles across the mainstream at different locations. The waves from upstream of the cavity are only partly compensated for by the rarefaction at the separation point. When no mass is added, the pressure remains approximately constant across the shear layer. As the purge flow in the upper cavity is turned on, the pressure increases and a gradient is established across the mainstream. For the higher flow rates, the pressure within the shear layer is no longer constant. The limited number of profiles suggests that the static pressure increases in flow direction, as to be expected, from the addition of momentum of the purge gas. This behavior needs further substantiation, because it may bear some negative implications with regard to maximum optical homogeneity of an otherwise improved flowfield. Besides this, the shear layer itself is an optically refractive element and may need independent consideration.

Conclusions

It has been demonstrated that cavity-induced flow distortions can be reduced by several techniques. The most efficient method is to enlarge the flow channel downstream of the cavity and balance the pressure drop by a matched purge flow. It might become necessary to trade off the advantage of a weak separation wave against a possible pressure increase along the cavity opening. Besides their general purpose of housing resonator elements, cavities may also be applied to prevent shock wave emanation from thermal boundary layers over wall electrodes.

Acknowledgments

The author is indebted to N. Döflinger and E. Wildermuth for their helpful assistance in performing the experiments and to Prof. H. Hügel for his valuable discussions.

References

[1]Petty, J.S., Cooper, J.R., and Korkegi, R.H., "The Use of Shaped Cavities to Improve the Sidewall Boundary Layer Quality in Gas Dynamic Lasers," ARL-TR 75-0024, March 1975.

[2]Shen, P., "Supersonic Flow over a Deep Cavity for a Laser Application," *AIAA Journal*, Vol. 17, Feb. 1979, pp. 216-219.

[3]Schall, W.O., "Einfluß von Kanalseitenkammern auf Strömungshomogenität und Laserleistung bei gasdynamischen Lasern," DFVLR-IB 441 473/84, 1984.

[4]Schall, W.O. and Dörflinger, N., "Disturbance of Supersonic Flow by Channel Side-Cavities," *Gas Flow and Chemical Lasers, 1984 Proceedings of 5th GCL Symposium*, Institute of Physics Conference Series, No. 72, Adam Hilger Ltd., Bristol, England, and Boston, 1985, pp. 451-456.

[5]Parazzoli, C.G., "Boundary Layer in a High Current Density Discharge," *AIAA Journal*, Vol. 15, June 1977, pp. 848-853.

[6]Bohn, W.L., Hügel, H., Schall, W.O., and Schock, W., "Vorrichtung zur Anregung und/oder Ionisierung eines fließenden Gases," FRG Patent Application DE 29 40 627, 1979.

[7]Mayerhofer, W., Hügel, H., and Novack, R., "Pulsed E-beam Stabilized Supersonic CO-Laser," *Gas Flow and Chemical Lasers, 1984 Proceedings of 5th GCL Symposium*, Institute of Physics Conference Series, No. 72, Adam Hilger Ltd., Bristol, England, and Boston, 1985, pp. 319-324.

Experimental Verification of Temperature Fluctuations During Combustion Instability

H. F. R. Schöyer,*
ESTEC, Noordwijk, The Netherlands
and
R. T. M. de Bont†
Delft University of Technology
Delft, The Netherlands

Introduction

In a recent paper[1] it was hypothesized that certain types of combustion instability might be caused by incomplete combustion. A consequence of this hypothesis is that for such oscillatory combustion, temperature fluctuations may be of the same order of magnitude as the pressure fluctations and may display the same behavior. It has also been suggested that for such oscillatory combustion, there are similar fluctuations in the composition of the combustion products. Eisel et al.[2] reported both fluctuations in the temperature and composition during L^* oscillations; Price[3] has reported variations in the composition of the exhaust during L^* instability, while Strand[4,5] and Kumar and McNamera[6] observed the occurrence of fluctuations in light intensity accompanying the pressure fluctuations during L^* instability. This note deals with the simultaneous measurement of temperature and pressure fluctuations during L^* instability.

Experiments

Disks of propellant, with a diameter of 10 cm and a thickness of about 1 cm, were burned in a variable volume, end-burning rocket motor. This L^* burner has been described elsewhere[7]. The nozzle end plate was made of two perspex disks to allow for the transmission of light and the visual observation of the combustion process. Different-size nozzles may be mounted. Ignition was achieved by means of a hot wire in combination with a pyrotechnic lacquer.[7] The combustion pressure was measured continuously by a Kistler piezoelectric transducer, mounted behind the propellant disk. Good contact between the transducer and the propellant was ensured by means of vaseline or silicon grease. The composition of the propellant was roughly: AP 74% (by weight), polyurethane 19.4%, aluminum 6%, and additives 0.6%. The theoretical flame temperature is about 2740 K. The Al and Al_2O_3 particles and droplets will act as blackbody radiators.

Temperature has been measured optically. To this end a 1-cm^2 United Detector Technology PIN-10 DF photocell was mounted in an SLR Hasselblad camera at the film position. The combination photocell-Hasselblad camera has been calibrated for various distances and apertures with the help of a tungsten-band lamp. In the region between 450 and 950 nm the light intensity is directly related to the blackbody temperature by a polynomial that may be obtained from Planck's radiation equation and a curve-fitting procedure.

The output of the photocell was amplified and subsequently digitized. The voltage output turned out to be very linear for light intensity ratios between 0.1 and 100. In applying this type of temperature measurement, the main uncertainty is the absorption of light by the perspex end plate.

Although the end plate remains transparent during combustion, particles and dirt are collected on the inner surface, while some perspex evaporates. To estimate the transparency of the end plate, a plate has been taken after a test run and the inner surface has been subsequently "wiped clean," after which it was determined that the transmissivity of the end plate was only 6.25% of the transmissivity of a "clean" end plate. This reduction in transmissivity has been assumed to be applicable during the major part of the test runs. As there is considerable uncertainty in this value, the measurements of the absolute temperature should not be regarded as fully reliable. On the other hand, the measurements of the relative temperature fluctuations $T'/\bar{T}$ do not suffer from this systematic error and may be regarded as being much more reliable.

During the actual experiments, a black screen was positioned between the camera and the L^* burner, preventing stray light from falling on the photocell. A small aperture in the screen ensures that only a small, well-defined portion of the nozzle end of the L^* burner is projected on the photocell.

The Hasselblad SLR camera allows for the precise determination of the dimensions of this area, so that it is known what portion of the photocell was actually covered. The outputs of the photocell and pressure transducer were recorded simultaneously on analog and digital magnetic tape and by a UV oscillograph for quick-look analysis. The voltage output of the photocell amplifier is in fact, a measure for the light intensity.

Results

According to Schöyer's hypothesis,[1] low-frequency combustion instability may be caused by incomplete combustion. Incomplete combustion itself should be accompanied by flame temperatures lower than the adiabatic flame temperature at complete combustion. The results indicate that the measured blackbody temperature is indeed lower than the theoretical adiabatic flame temperature. As mentioned previously, the measured value of the blackbody temperature may not be ac-

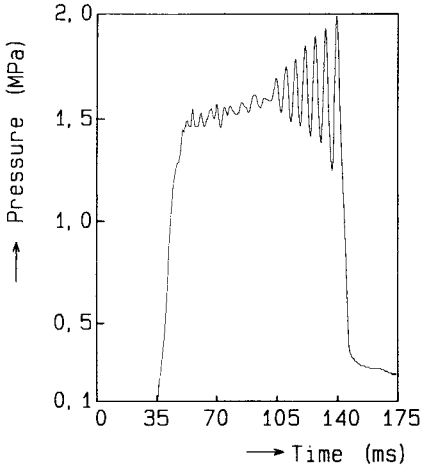

Fig. 1 A typical pressure record during L^* instability.

Received Dec. 17, 1984; revision received March 20, 1985.

*Propulsion Engineer, Mechanical Systems Division. Member AIAA.

†Graduate Student, Department of Aerospace Engineering.